

# Strain Induced Superconductivity of RuO<sub>2</sub>

Kedar Johnson<sup>1, 2</sup>, Luka Mitrovic<sup>3</sup>, Darrel G. Schlom<sup>3</sup>

<sup>1</sup>Clark Atlanta University, Department of Physics, Atlanta, Georgia

<sup>2</sup>Morehouse College, Dual Degree Engineering Program, Atlanta, Georgia

<sup>3</sup>Cornell University, Department of Material Science, Ithaca, New York

## Abstract

Applying *c* axis compressive strain is a method for promoting superconductivity in Ruthenium Dioxide (RuO<sub>2</sub>) that is still being studied. Prior research discovered this relationship between *c*-axis compression in RuO<sub>2</sub> and its superconductive properties when it was grown on Titanium Dioxide (TiO<sub>2</sub>) substrates that achieved a 4.7% *c* axis lattice mismatch in the sample.<sup>2</sup> The focus of our research is to further study this relationship promoting superconductivity by testing RuO<sub>2</sub> growths on other substrates that can create a similar degree of lattice mismatch. Qualifying substrates must have a similar enough lattice structure to RuO<sub>2</sub> to apply strain within an effective range, the exact limits of which must also be tested.<sup>1</sup> The only substrates tested prior have been similar commercially available rutiles,<sup>2</sup> so our research contained some more exotic substrates namely synthetic alexandrite (Al<sub>2</sub>BeO<sub>4</sub>). Our results identify the feasibility of using synthetic alexandrite as a substrate for producing a strain induced superconductive state in RuO<sub>2</sub>.

## Introduction

Ruthenium dioxide (RuO<sub>2</sub>) is a metal compound which was discovered to be able to enter a superconductive state while its lattice structure is under *c* axis compression.<sup>2</sup> Note that prior to this method, RuO<sub>2</sub> has not been known to exhibit superconductivity. Previous studies at Cornell by J. P. Ruf, et al. (2021) discovered this relation between superconductivity and *c* axis compression by growing RuO<sub>2</sub> on titanium dioxide (TiO<sub>2</sub>) substrates in various orientations.<sup>2</sup> Superconductivity was observed from samples grown on TiO<sub>2</sub> in (110) and (100) orientations when their resistivity dropped to 0 μΩ•cm after being reduced to a temperature of 1.8 K.<sup>2</sup> This phenomenon was not observed in other compared samples: RuO<sub>2</sub> on TiO<sub>2</sub> (101) and bulk RuO<sub>2</sub>.<sup>2</sup> Analysis of the RuO<sub>2</sub> on TiO<sub>2</sub> (110) and (100) samples identified a 4.7% *c* axis lattice mismatch in contrast to the much less strained alternate samples.<sup>2</sup> Similar research was conducted with magnesium difluoride (MgF<sub>2</sub>), however no RuO<sub>2</sub> on MgF<sub>2</sub> samples exhibited superconductivity.

The only two substrates that have been used to support the growth of superconducting RuO<sub>2</sub> are TiO<sub>2</sub> and MgF<sub>2</sub>, as they are the only two existing commercially available rutile substrates.<sup>2, 3</sup> Our research focused on some more exotic non rutile substrates: synthetic topaz (Al<sub>2</sub>SiO<sub>4</sub>[F, OH]<sub>2</sub>) and synthetic alexandrite (Al<sub>2</sub>BeO<sub>4</sub>) which will be referred to as topaz and alexandrite onward.<sup>3</sup> Both of these compounds have orthorhombic unit cells, more ideal octahedral alignment, and favorable lattice mismatch.<sup>1, 3</sup> The report from this point forward focuses on RuO<sub>2</sub> (001) on alexandrite (100) as our RuO<sub>2</sub> (001) on topaz samples did not yield the strain and other results we were looking for. For these samples *c* axis compression was accomplished using the Poisson effect.

## Methods

Samples were grown via molecular beam epitaxy (MBE). A ruthenium source was evaporated by electron beam and deposited on the substrate while within an ozone background for RuO<sub>2</sub> formation during deposition. RHEED imaging was used to monitor the sample's growth and the formation of its crystal structure. Growth temperatures for 8

samples in a temperature focused series included 350 °C, 300°C, 250 °C, 225 °C, 200 °C, 175°C, 150°C, and 100 °C. The samples grown at 225 °C and 175 °C were grown in response to the measurements seen for the sample grown at 200 °C. No polycrystallinity was seen at lower temperatures according to RHEED (see Fig. 1).

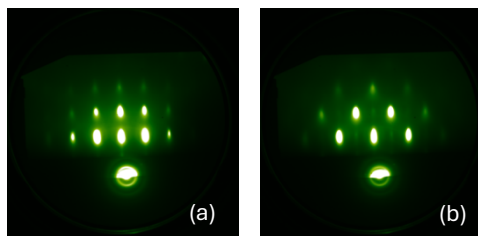


**Fig. 1** (a) and (b) are RHEED images from growth of RuO<sub>2</sub> (001) on alexandrite (100). This rough pattern is consistent with other rutile films grown in the (100) orientation, and they show the absence of polycrystallinity.

Sample film thickness and surface quality for each sample in the thickness series were then measured via x-ray reflectivity (XRR). For this research, surface quality is a more arbitrary variable that is included to show the relative clarity in XRR readings when comparing RuO<sub>2</sub> (001) on Alexandrite (100) to RuO<sub>2</sub> (001) on TiO<sub>2</sub> (001). The ladder only reliably shows the first two Laue fringes, which is enough to determine film thickness, but does not provide as reliable information pertaining to the surface quality as the former (see Fig. 3). X-ray diffraction (XRD) was done soon after to analyze the atomic structure and assess the amount of *c*-axis compression observed in the temperature series samples (see Fig. 2). The sample grown at 200 °C was found to exhibit the most *c* axis compression with its RuO<sub>2</sub> 002 peak recorded at a 2θ of 60.26 °C. Further data for the temperature series focuses on this sample.

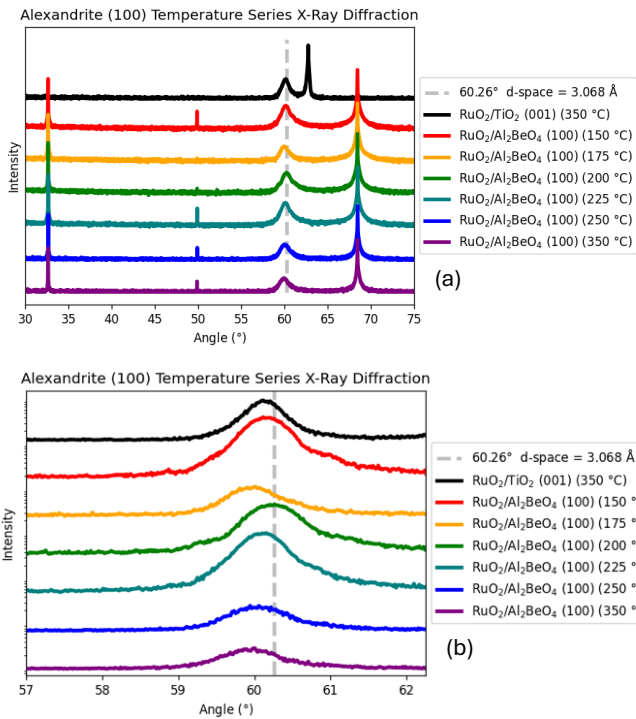


**Fig. 2** (a) and (b) are plots of the XRD measurements at the RuO<sub>2</sub> 002 peak of the RuO<sub>2</sub> (001) on Alexandrite (100) temperature series samples. RuO<sub>2</sub> on TiO<sub>2</sub> is included in black for comparison. A dotted line marks the 2θ angle for the RuO<sub>2</sub> 002 peak of the 200 °C sample at 60.26°. Fig. 2(b) is a focused on the RuO<sub>2</sub> 002 peak.

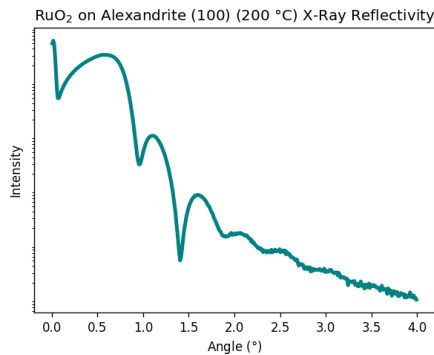


**Fig. 3** Plot of the XRR measurement of RuO<sub>2</sub> (001) on Alexandrite (100) grown at 200 °C. This plot indicates a film thickness of approximately 14.7 nm.

Reciprocal space mapping (RSM) was then completed on the 200 °C sample (see Fig. 4). The RSM results showed that the film peak was in line with the substrate peak which indicates commensurate strain, however the dispersion of the film peak showed that the sample was grown beyond the onset of relaxation. Historically, thinner samples are closer to or precede the onset of relaxation, therefore, we should test growing thinner samples at the same 200 °C growth temperature.

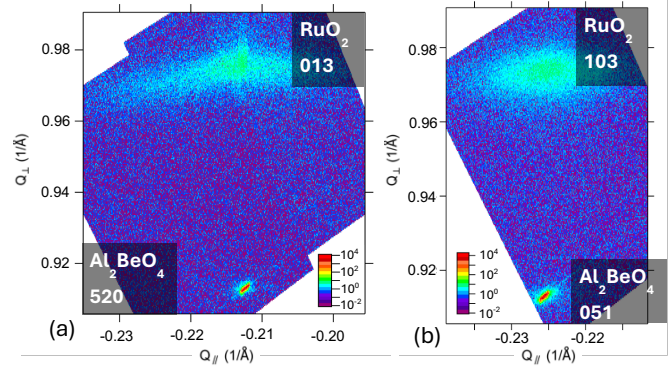


**Fig. 4** (a) and (b) are RSM graphs of RuO<sub>2</sub> (001) on Alexandrite (100) grown at 200 °C and 14.7 nm. (a) is measured at the RuO<sub>2</sub> 013 peak and (b) is measured at the RuO<sub>2</sub> 103 peak.

Further measurements for this sample included physical property measurement system (PPMS) transports (see Fig. 5) and rocking curve scans (see Fig. 6). The PPMS transport shows that the RuO<sub>2</sub> (001) on Alexandrite (100) 200 °C sample has a metallic nature as resistivity does decrease with the decreasing temperature. There was no observed superconductivity as resistivity did not drop to zero down to 1.8 K, hence, there was no indication of a critical temperature. Rocking curve scans for this sample showed a high crystal quality despite the high strain. This is represented by less noise and a small full width half max (FWHM).

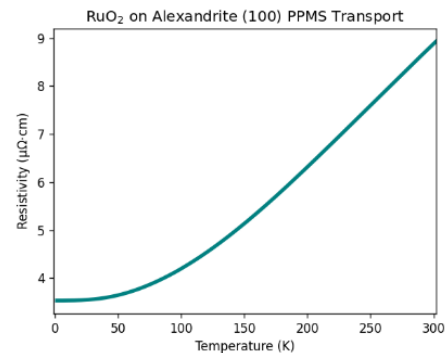


**Fig. 5** PPMS transport plot of RuO<sub>2</sub> (001) on Alexandrite (100) grown at 200 °C and 14.7 nm. Lowest recorded resistivity at 1.8 K was 3.534 μΩ•cm.

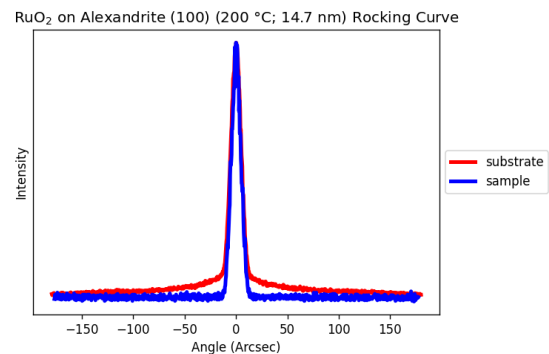


**Fig. 6** Rocking curve plot of RuO<sub>2</sub> (001) on Alexandrite (100) grown at 200 °C and 14.7 nm. Full width half max (FWHM) for the film is 10.44 arcsec and for the substrate is 11.88 arcsec.

Following the temperature series, we completed a thickness series of RuO<sub>2</sub> (001) on Alexandrite (100) samples grown at 200 °C. Along with the original sample, which had a film thickness of 14.7 nm, two more samples were grown with 7.5 nm and 5 nm thick films. Another set of XRD measurements (see Fig. 7) and XRR measurements (see Fig. 8) were completed to compare with the original 200 °C sample. The XRD plots of the thickness series showed that the RuO<sub>2</sub> 002 peak for all three samples were at the same 2θ, thus, they were observed as having equal c-axis compression. The XRR plots for the thickness series had the same trend as the original 14.7 nm sample where their XRR measurements had higher relative clarity compared to RuO<sub>2</sub> (001) on TiO<sub>2</sub> (001).

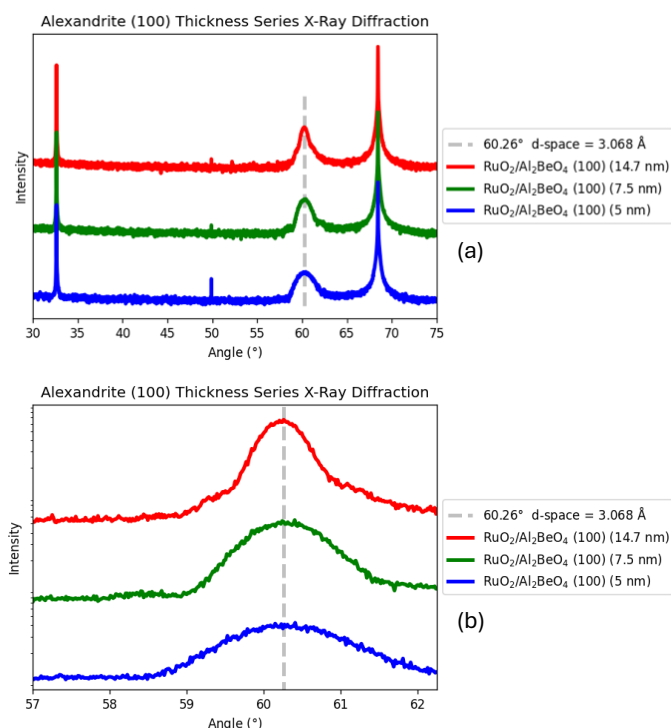


**Fig. 8** (a) and (b) are XRD measurements of the RuO<sub>2</sub> (001) on Alexandrite (100) samples grown at 200 °C in the thickness series. The dotted line marks the RuO<sub>2</sub> 002 peak at a 2θ of 60.26°.

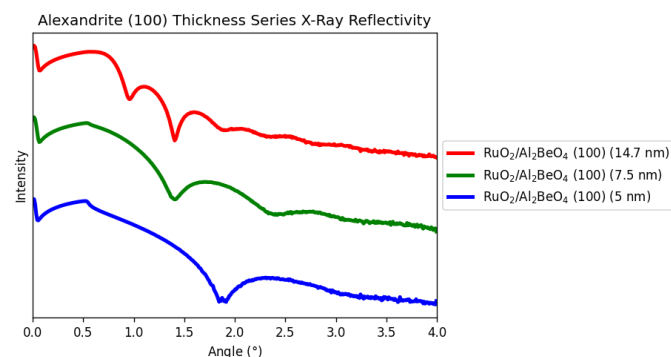


**Fig. 9** XRR measurements of the RuO<sub>2</sub> (001) on Alexandrite (100) samples grown at 200 °C in the thickness series.

RSMs were taken for the 7.5 nm and 5.0 nm samples in the thickness series (see Fig. 10 and Fig. 11) and

were compared to the original 14.7 nm sample. The dispersion at the film peaks grew smaller with each thinner sample and reached a point much nearer to the onset of relaxation (potentially before the onset). The RSMs for the thinner samples agreed with XRD in that there was no significant change to the c axis compression with respect to the decreased film thickness.

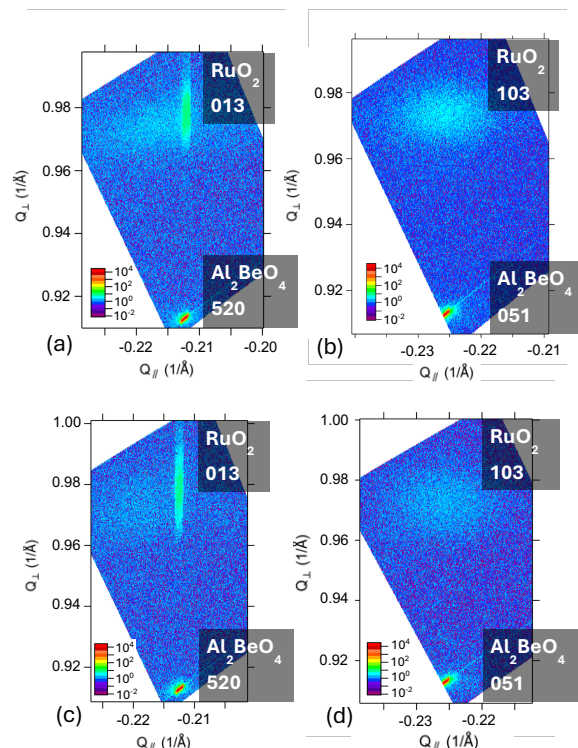


**Fig. 10** RSM measurements of the RuO<sub>2</sub> (001) on Alexandrite (100) samples grown at 200 °C with film thicknesses of 7.5 nm and 5.0 nm. (a) is measured at the RuO<sub>2</sub> 013 peak and (b) is measured at the RuO<sub>2</sub> 103 peak for the 7.5 nm sample. (c) is measured at the RuO<sub>2</sub> 013 peak and (d) is measured at the RuO<sub>2</sub> 103 peak for the 5.0 nm sample.

## Results

RuO<sub>2</sub> (001) on Alexandrite (100) reached a peak c axis compressive strain at roughly 200 °C. Varying the film thickness had no significant effect on the compression. RuO<sub>2</sub> (001) on Alexandrite (100) exceeded the c axis compressive strain and surface quality of RuO<sub>2</sub> (001) on TiO<sub>2</sub> (001) and RuO<sub>2</sub> (001) on MgF<sub>2</sub> (001), however, no superconductivity was observed down to 1.8 K. Continuing forward, more PPMS transports will need to be completed down to 0.4 K with the use of Helium-3 to confirm that no suppressed critical temperature is present. Further research will investigate growing other rutile oxides on alexandrite (100) including Iridium Dioxide.

## References

1. Raja, P. M. V. & Barron, A. R. in *Physical Methods in Chemistry and Nano Science* (Rice University, 2012).
2. Ruf, J. P. *et al.* Strain-stabilized superconductivity. *Nature Communications* **12**, (2021).
3. Zagorac, D., Muller, H., Ruehl, S., Zagorac, J. & Rehme, S. J. ICSD-34064 (ICSD release 2024.1)